

## DISCOVERY OF HIGH-DEGREE NONRADIAL OSCILLATIONS IN RAPIDLY ROTATING $\delta$ SCUTI STARS?

G. A. H. WALKER,<sup>1</sup> S. YANG,<sup>1</sup> AND G. G. FAHLMAN

Department of Geophysics and Astronomy, University of British Columbia

Received 1987 April 16; accepted 1987 June 29

### ABSTRACT

We obtained time-resolved spectral series ( $\sim P/10$ ) covering a single photometric period in the region of  $\lambda 4500$  for four rapidly rotating ( $\sim 120 \text{ km s}^{-1}$ )  $\delta$  Scuti stars. In all four cases the line profiles show the unmistakable signature of traveling subfeatures already seen in Spica and  $\zeta$  Ophiuchi, where they have been attributed to high-degree nonradial pulsations. The weaker lines tend to be more strongly modulated than the stronger ones. The subfeatures are not always quite equally spaced, and they can show phase changes and doubling reminiscent of the extreme  $\beta$  Cephei stars.

On the simplifying assumption that the subfeatures are periodic and can be ascribed to a nonradial, spherical harmonic motion with  $l = |m|$ , and that stellar rotation dominates the acceleration, we calculate values of  $|m| = 8, 14, 16, 16$  (with typical standard deviations of 20%) for 21 Mon,  $\kappa^2$  Boo,  $\nu$  UMa,  $\sigma^1$  Eri, respectively. For 21 Mon and  $\kappa^2$  Boo the values of  $\Delta t$  are close to the dominant photometric period, but closer to half the photometric period for the other two stars. The value of  $\Delta t$ , the average time delay between subfeatures, for  $\sigma^1$  Eri is identical to that derived from observations at  $\lambda 8700$  in 1983.

If attribution of the moving subfeatures to high-degree, nonradial motions is correct, this discovery now extends its known occurrence to the  $\delta$  Scuti variables.

*Subject headings:* stars: individual ( $\sigma^1$  Eri,  $\kappa^2$  Boo,  $\nu$  UMa, 21 Mon) — stars: pulsation — stars: variables

### I. INTRODUCTION

The  $\delta$  Scuti variables have pulsation periods of less than 0<sup>d</sup>.3, are of spectral types A or F, and generally lie above the main sequence. Good reviews can be found in Breger (1979) and Wolff (1983). Smith (1982) found that nonradial harmonic indices of  $l \leq 2$  gave the best fitting line profiles for five  $\delta$  Scuti stars. Recently, Yang and Walker (1986) presented evidence of nonradial pulsation of a high-degree ( $m \approx 14$ ) for the  $\delta$  Scuti variable  $\sigma^1$  Eridani. They saw subfeatures moving through the rotationally broadened lines of Ca II  $\lambda 8662$  and Fe I  $\lambda 8689$ .

Stellar rotation broadens an intrinsically sharp absorption line. Contributions to the line profile from longitudinal strips on the stellar disk are displaced from the line center by their projected velocity which transforms the line profile into a one-dimensional “Doppler view” of the stellar disk. Velocity perturbations caused by motions whose phase is a function of longitude (nonradial) displace the contributions of the various longitudinal strips causing bumps and dips in the line profile. These features are carried by rotation and wave motion through the line profile. Such traveling subfeatures have been seen in the absorption lines of the  $\beta$  Cephei variable Spica by Walker *et al.* (1982), Smith (1985a), and Fahlman *et al.* (1987); in the rapidly rotating O star  $\zeta$  Ophiuchi by Walker, Yang, and Fahlman (1979), and Vogt and Penrod (1983); and

in the Be shell star  $\gamma$  Cassiopeia by Ninkov, Yang, and Walker (1983). Vogt and Penrod (1983) reproduced the subfeatures in  $\zeta$  Ophiuchi with model profiles distorted by nonradial oscillations with equal harmonic and azimuthal wavenumbers for the associated spherical harmonic (i.e.,  $l = |m|$ ). Smith (1985b) and Fahlman *et al.* (1987) have found a similar solution for Spica.

In Spica the nonradial oscillations apparently have a prograde motion parallel to the equator with a phase velocity which is only about 10% of the rotational velocity. When the phase velocity is small compared to the rotational velocity, one can estimate an approximate value of  $|m|$  and the rotational period,  $P_{\text{rot}}$ , from the relations:

$$|m| = 2\pi(v \sin i)/(a_0 \Delta t) \quad (1)$$

$$P_{\text{rot}} = |m| \Delta t, \quad (2)$$

where  $a_0$  and  $\Delta t$  are the acceleration at the line center and the average delay between the subfeatures, respectively (see Yang and Walker 1986). This technique essentially amounts to counting the number of nonradial oscillation cycles around the star.

While the velocity perturbations introduced by nonradial motions provide a satisfactory description of the observations, there is no agreement about the underlying mechanism which could sustain them or the range of spectral types and luminosities over which they occur (Cox 1984). While azimuthal temperature fluctuations could also generate similar subfea-

<sup>1</sup>Visiting Astronomer, Canada-France-Hawaii Telescope operated by the National Research Council of Canada, the Centre National de la Recherche Scientifique of France, and the University of Hawaii.

TABLE 1  
THE  $\delta$  SCUTI VARIABLES: OBSERVATIONS AND  $|m|$

Parameter	21 Mon	$\kappa^2$ Boo	$\nu$ UMa	$\sigma^1$ Eri
Sp type	A8 Vn	A8 IV	F2 IV	F2 II-III
$v \sin i$ (km s $^{-1}$ )	121	127	110	96
$P_{\text{phot}}$ (days)	0.10	0.066	0.132	0.081
Exposure time (s)	850	525	800	500
$T$ (days)	0.115	0.099	0.160	0.181, 0.087
$S/N$ per diode	227	450	820	544
$\Delta t$ (days)	0.104	0.045	0.066	0.047
$a_0$ (km s $^{-1}$ d $^{-1}$ )	925	1280	660	800
$P_{\text{rot}}$ (days)	0.82	0.62	1.05	0.75
$ m $	8	14	16	16

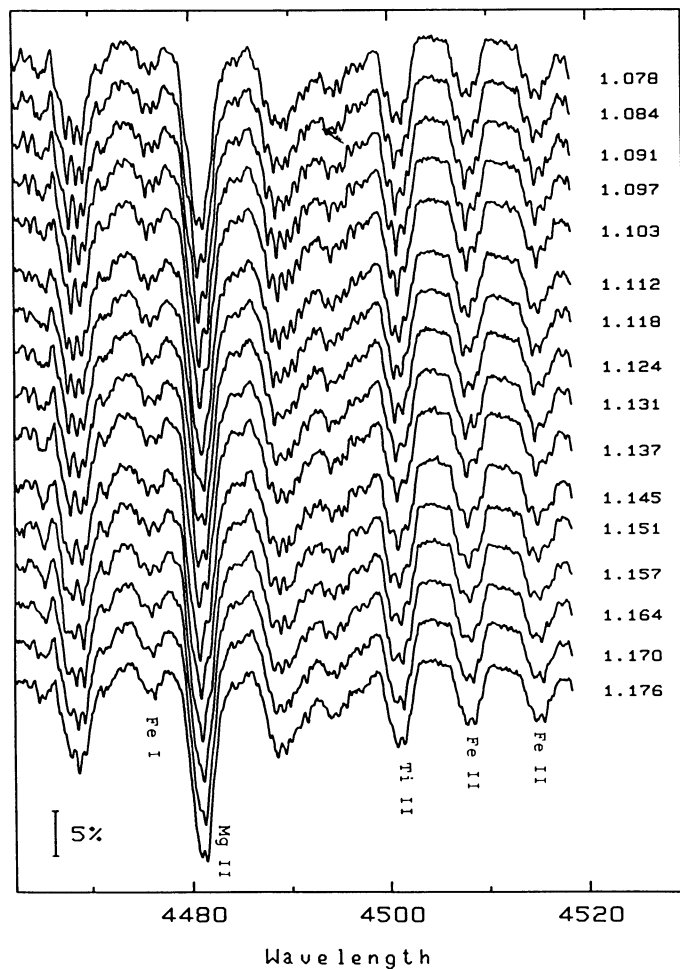


FIG. 1.—Spectral time series for  $\kappa^2$  Boo. The numbers at the right are fractions of the barycentric JD 2,446,838. The moving subfeatures are best seen with the eye almost in the plane of the page. Some of the stronger stellar absorption lines are identified.

tures, our observations show, that in some stars, particularly  $\sigma^1$  Eri, the subfeatures regularly broaden and divide in a way which is difficult to model credibly by temperature variations alone.

Our discovery of apparent, high-degree, nonradial pulsations in  $\sigma^1$  Eridani was the first for an F star, which probably

has a convective envelope and which may have important implications both for stellar structure and the excitation mechanism. It seemed important to us both to confirm the result for  $\sigma^1$  Eridani and to test its uniqueness by observing other rapidly rotating  $\delta$  Scuti variables with high time and spectral resolution.

We were awarded two nights for the program on the Canada-France-Hawaii Telescope in 1987 February and chose to observe at  $\lambda 4500$  where the spectrum is rich in absorption lines and there is a higher photon flux than at  $\lambda 8700$ . Apart from confirming the result for  $\sigma^1$  Eridani, we found clear evidence of moving subfeatures in the lines of each of the other three stars. It is the purpose of this *Letter* to communicate this important result. We shall publish a detailed analysis and comparisons with model line profiles later for each star.

## II. OBSERVATIONS

Details of the program stars, the observations, and the derived quantities are given in Table 1. The dominant photo-

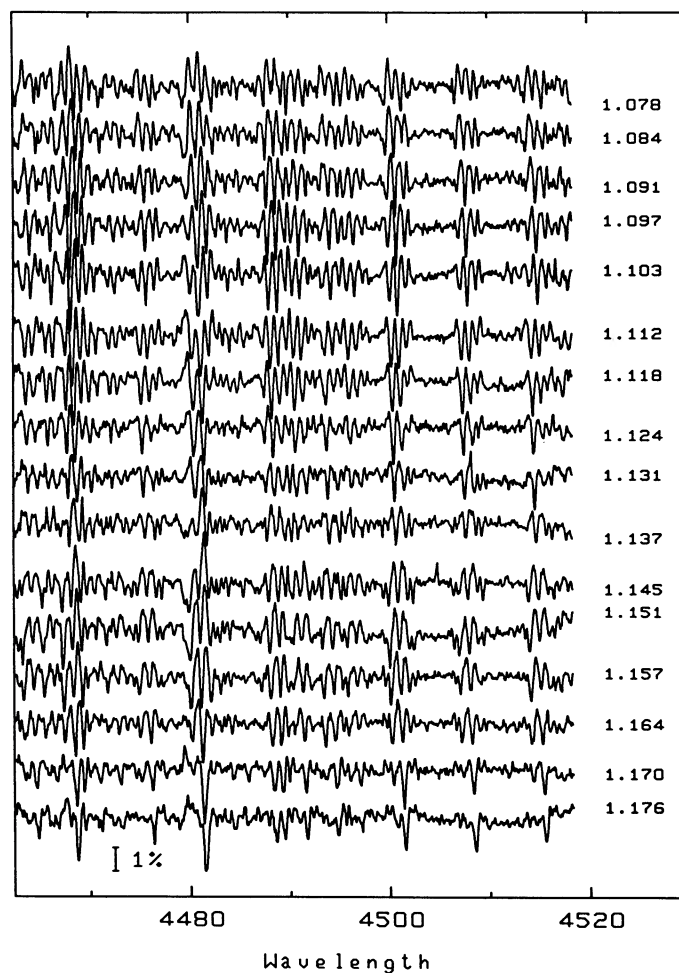


FIG. 2.—Time series of residuals for  $\kappa^2$  Boo formed by taking the difference between the spectra in Fig. 1 and the mean spectrum from the time series. The residuals emphasise the moving subfeatures. Note that the weaker lines in Fig. 1 show a larger relative modulation than the strong lines. Line blending introduces the phase shifts in the ripple pattern.

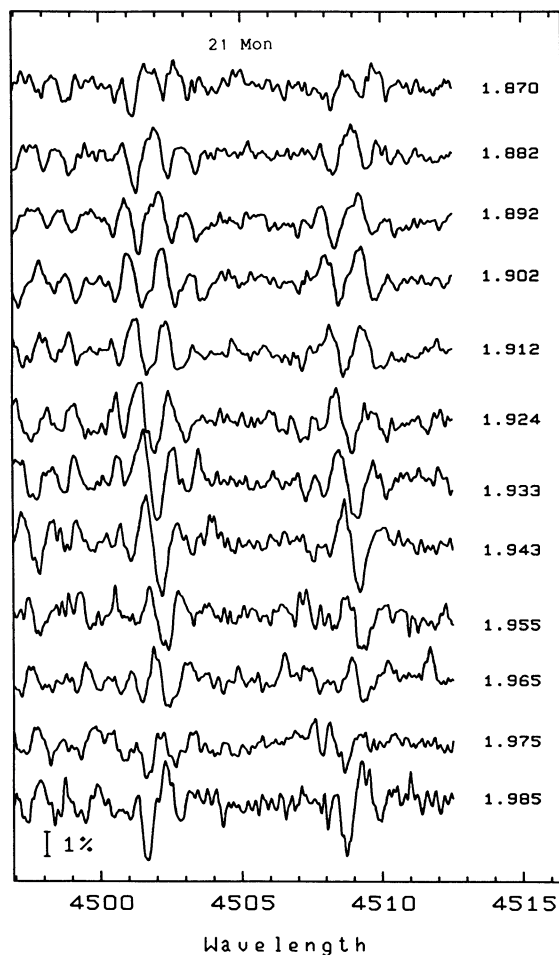


FIG. 3a

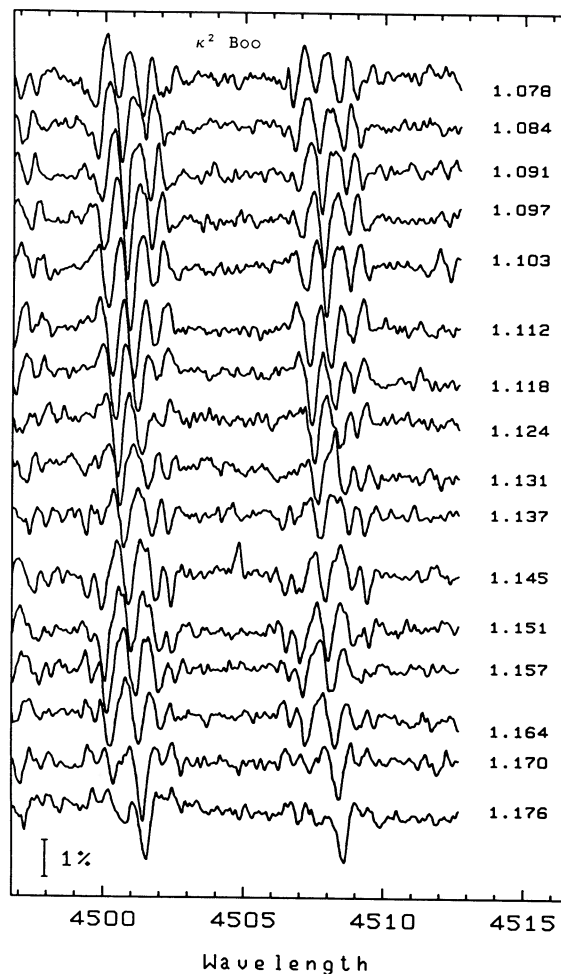


FIG. 3b

FIG. 3.—As Fig. 2 for all four of the program stars for the largely unblended lines of Ti II  $\lambda$ 4501 and Fe II  $\lambda$ 4508

metric periods,  $P_{\text{phot}}$ , have been taken from Breger (1979),  $v \sin i$ , spectral types, and luminosity classes are from Hoffleit and Jaschek (1982). The exposure time is the average per spectrum;  $T$  is the total length of the time series expressed as a fraction of a day ( $\alpha^1$  Eri was observed on both nights);  $S/N$  is the average signal-to-noise ratio per sample point in the unsmoothed, processed spectra. The acceleration of the subfeatures at the line center,  $a_0$ , and  $\Delta t$ , the average time delay between the subfeatures, were both measured from plots such as that shown in Figure 4. The values of  $|m|$  are derived from equation (1) and  $P_{\text{rot}}$  from equation (2).

The stars were observed on the nights of 1987 February 12 and 13 (UT) with the f/8.2 camera of the coude four-grating-mosaic spectrograph (Brealey *et al.* 1980) using a refrigerated RL1872F/30 EG & G Reticon as detector (Walker, Johnson, and Yang 1985). The grating, blazed at  $\lambda 8000$ , gives a reciprocal dispersion in the second order of  $2.4 \text{ \AA mm}^{-1}$  at  $\lambda 4500$ . This corresponds to a dispersion close to  $0.035 \text{ \AA}$  per pixel on the Reticon array and a spectral coverage of  $65 \text{ \AA}$ . Observations were possible for all but the last half-hour on the first night but for only half of the second night when they were also limited by high winds and intermittent cloud.

Thorium/neon arcs were recorded once an hour to calibrate wavelength drifts in the equipment. "Flat-field" incandescent lamp spectra were recorded with the lamp illumination filling the same telescope exit pupil as the star. The position of the exit pupil was isolated with a diaphragm and adjusted when necessary for each star. The data were reduced with the program RETICENT (Pritchett, Mochneck, and Yang 1982). The technique of preprocessing the Reticon spectra to obtain the optimum  $S/N$  has been described in Walker, Johnson, and Yang (1985).

### III. THE LINE PROFILE VARIATIONS

There are too many data to present in a brief *Letter*. We shall restrict ourselves to examples which outline the reduction technique. Figure 1 shows the spectral time series for  $\kappa^2$  Boo. The numbers to the right of each spectrum correspond to the midexposure time expressed as a fraction of the barycentric Julian Day 2,446,838. Midexposure times weighted by the output of the exposure meter were calculated automatically to within 5 s. The principal spectral lines are identified. The original spectra were normalized both with an incandes-

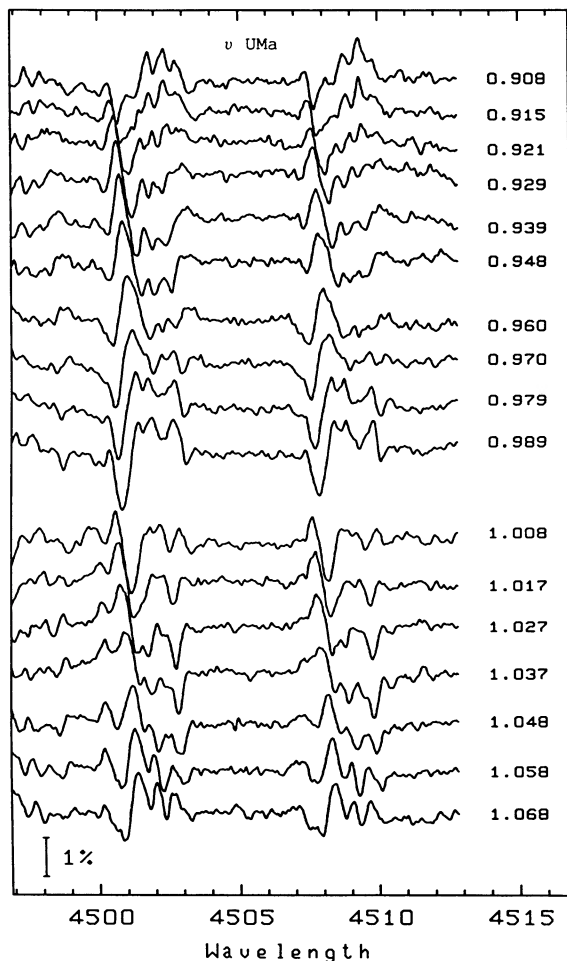


FIG. 3c

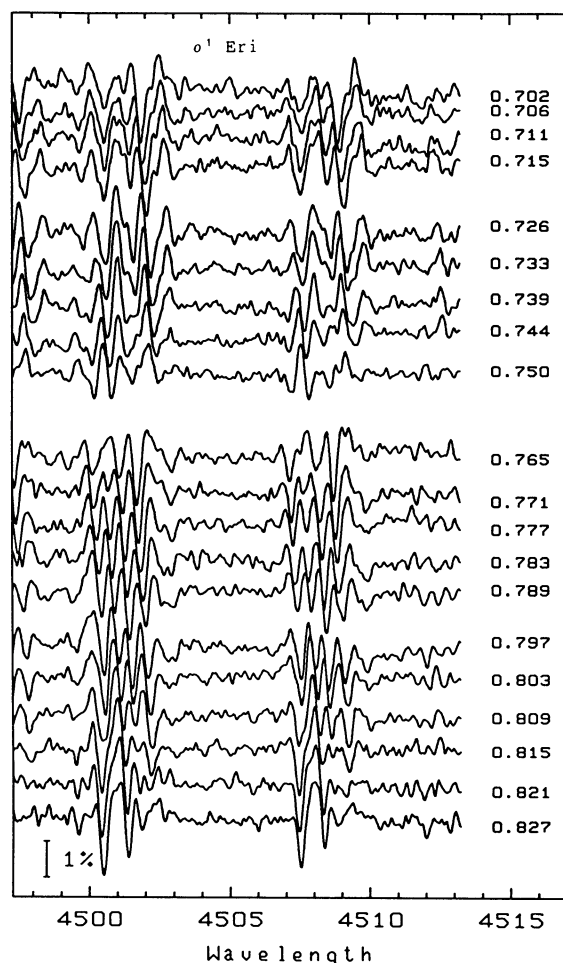


FIG. 3d

FIG. 3—Continued

cent lamp spectrum and to a continuum defined by a low-order polynomial. The latter eliminates residual spectral curvature. The spectra have been smoothed with a Gaussian profile having  $\sigma = 0.042 \text{ \AA}$ .

Subfeatures are very obvious as ripples running through all the lines and are best seen with the eye almost in the plane of the page. The subfeatures are shown in high contrast in Figure 2 where residuals, generated by taking differences between the individual spectra and the mean spectrum for the time series, are plotted. Such a plot is insensitive to nonvarying features in the line profiles such as rotational broadening. The modulation of the weaker lines appears to be greater than that of the stronger lines which is also a characteristic of the early-type stars in which nonradial oscillations have been seen. The net effect of this inverse dependence on line strength and the many blended lines is the appearance of an almost continuous ripple traveling through each of the residual spectra.

#### IV. $|m|$ , $\Delta t$ , $P_{\text{phot}}$ , NONRADIAL PULSATIONS?

Figure 3 shows the time series of the residuals for each of the stars in the neighborhood of the  $\lambda 4508 \text{ Fe II}$  line and  $\lambda 4501 \text{ Ti II}$  lines. These lines are of moderate strength in all of

the spectra but sufficiently free of blends to avoid interference effects from neighboring lines. Each plot of residuals in Figure 3 has an individual character with the pattern for  $\kappa^2 \text{ Boo}$  perhaps bearing the closest resemblance to that expected for a classical, smooth, running-wave pattern from a nonradial oscillation with purely radial motions.

The values of  $a_0$  and  $\Delta t$  given in Table 1 are based entirely on measurements of the  $\lambda 4508 \text{ Fe II}$  line. The accelerations of the six obvious subfeatures for  $\kappa^2 \text{ Boo}$  in Figure 3 are plotted in Figure 4. The different features are distinguished by different symbols and the best fitting straight lines are shown. The value of  $a_0$  corresponds to the average gradient for the two subfeatures which cross the line center during the series.  $\Delta t$  was estimated from the average delay between the straight lines.

Although the straight lines satisfactorily represent the data, there are systematic departures of the observations from them which are easily seen by sighting along the subfeatures in Figure 3. In Spica, Fahlman *et al.* (1987) explain these second-order effects by azimuthal motions having similar velocity amplitudes to the radial component of the motion. However, it should be stressed that the time series for each star covers only about one photometric cycle. It can be seen from

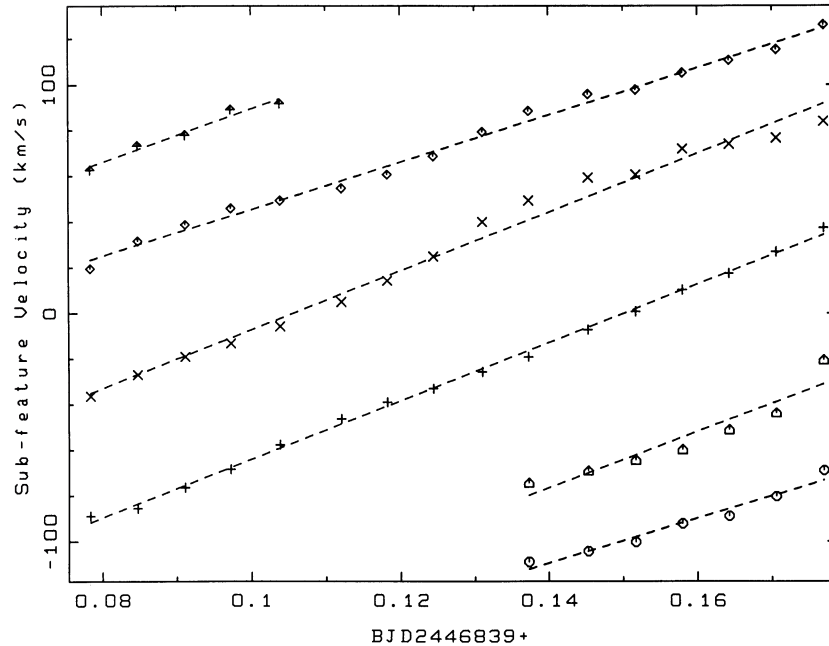


FIG. 4.—Acceleration of the six obvious subfeatures in Fig. 3 for  $\kappa^2$  Boo

Table 1 that  $\Delta t$  is either equal to, or half of, the photometric period. As a result, the mean profiles from which the residuals are formed in Figures 2 and 3 are not independent of the detected subfeatures since the latter only move of the order of twice their width during the series. This causes systematic effects of phase, amplitude, and profile through the series. The time series should be several times longer than the photometric period to provide a more independent mean.

Accelerations and time delays were measured for all of the stars as described above for  $\kappa^2$  Boo. The values derived from equation (1) for  $|m|$  are 7.9, 13.8, 15.9, and 16.0 for 21 Mon,  $\kappa^2$  Boo,  $\nu$  UMa, and  $o^1$  Eri, respectively. Rounded-off values are given in Table 1. While the coincidences with integral, even numbers is striking, the uncertainties associated with  $\nu \sin i$ ,  $a_0$ , and  $\Delta t$  suggest a standard deviation of order 20% in  $|m|$ .

In addition to the suggestive numbers for  $|m|$  there is additional support for the subfeatures being due to some periodic, nonradial, motion of the stellar surface. The values of  $\Delta t$  are very similar to  $P_{\text{phot}}$  for 21 Mon and  $\kappa^2$  Boo and to half  $P_{\text{phot}}$  for  $\nu$  UMa and  $o^1$  Eri (where  $|m| = 16$ ). For  $o^1$  Eri,  $\Delta t$  is actually closer to half of the mean period of  $0^d.088$

found by Yang and Walker (1986) for the radial velocity curve of the  $\lambda 8662$  Ca II line. The value of  $\Delta t$  which they found from the subfeatures in the Fe I  $\lambda 8689$  line,  $0^d.047$ , is identical to the value we have found 4 yr later at  $\lambda 4508$ .

The residuals in Figure 4 and the associated acceleration plots are not entirely consistent with purely radial periodic motions with a single phase velocity. For one thing, the features are not equally spaced; the values of  $\Delta t$  given in Table 1 are an average. One of the subfeatures particularly near 0.74 for  $o^1$  Eri broadens and divides and there are marked departures from uniform acceleration near the line center. The latter could be due to azimuthal motions while the former, also visible in the residuals for  $\nu$  UMa, are strongly reminiscent of the velocity stillstand in such extreme  $\beta$  Cephei stars as BW Vulpeculae (Goldberg, Walker, and Odgers 1976) when a high-velocity “atmosphere” and underlying “surface” seem to be visible simultaneously. It is almost certain that the apparent nonradial oscillations reported here are a first-order approximation to a more complex underlying motion.

This research was supported with funds from the Natural Sciences and Engineering Research Council of Canada.

#### REFERENCES

- Brealey, G. A., Fletcher, J. M., Grundman, W., and Richardson, E. H. 1980, *Proc. Soc. Photo-Opt. Instr. Eng.*, **240**, 225.  
 Breger, M. 1979, *Pub. A.S.P.*, **91**, 5.  
 Cox, J. P. 1984, *Pub. A.S.P.*, **96**, 577.  
 Fahlman, G. G., Francis, D., Fraser, G., Thibault, D., Walker, G. A. H., and Yang, S. 1987, preprint.  
 Goldberg, B. A., Walker, G. A. H., and Odgers, G. J. 1976, *A.J.*, **81**, 433.  
 Hoffleit, D., and Jashchek, C. 1982, *The Bright Star Catalogue* (New Haven: Yale University Observatory).  
 Ninkov, Z., Yang, S., and Walker, G. A. H. 1983, *Hvar Obs. Bull.*, **7**, 167.  
 Pritchett, C. J., Mochnacki, S., and Yang, S. 1982, *Pub. A.S.P.*, **94**, 733.  
 Smith, M. A. 1982, *Ap. J.*, **254**, 242.  
 Smith, M. A. 1985a, *Ap. J.*, **297**, 206.  
 ———. 1985b, *Ap. J.*, **297**, 224.  
 Vogt, S. S., and Penrod, G. D. 1983, *Ap. J.*, **275**, 661.  
 Walker, G. A. H., Johnson, R., and Yang, S. 1985, in *Adv. Electronics Electron Phys.*, **64A**, 213.  
 Walker, G. A. H., Moyle, K., Yang, S., and Fahlman, G. G. 1982, *Pub. A.S.P.*, **94**, 143.  
 Walker, G. A. H., Yang, S., and Fahlman, G. G. 1979, *Ap. J.*, **233**, 199.  
 Wolff, S. C. 1983, in *The A-Stars: Problems and Perspectives* (NASA SP-463), p. 93.  
 Yang, S., and Walker, G. A. H. 1986, *Pub. A.S.P.*, **98**, 1156.

G. G. FAHLMAN, G. A. H. WALKER, and S. YANG: Geophysics and Astronomy Department, University of British Columbia, Vancouver, B. C. V6T 1W5, Canada